

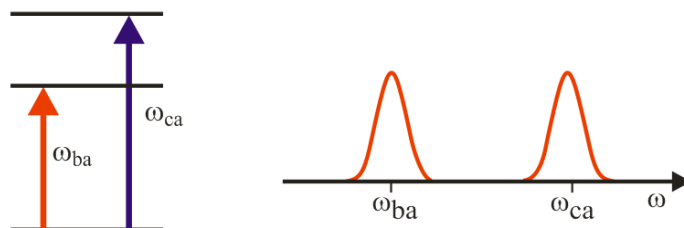
MIT OpenCourseWare  
<http://ocw.mit.edu>

5.74 Introductory Quantum Mechanics II  
Spring 2009

For information about citing these materials or our Terms of Use, visit: <http://ocw.mit.edu/terms>.

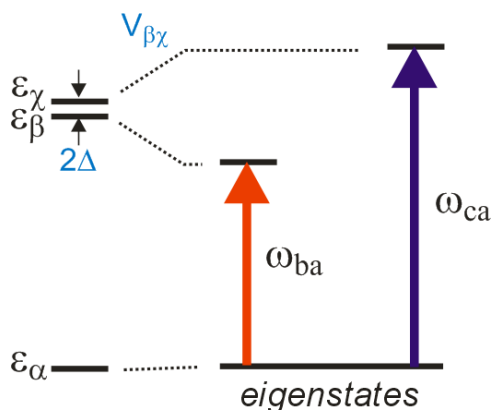
## 11.6. TWO-DIMENSIONAL CORRELATION SPECTROSCOPY

Our examination of pump-probe experiments indicates that the third-order response reports on the correlation between different spectral features. Let's look at this in more detail using a system with two excited states as an example, for which the absorption spectrum shows two spectral features at  $\omega_{ba}$  and  $\omega_{ca}$ .

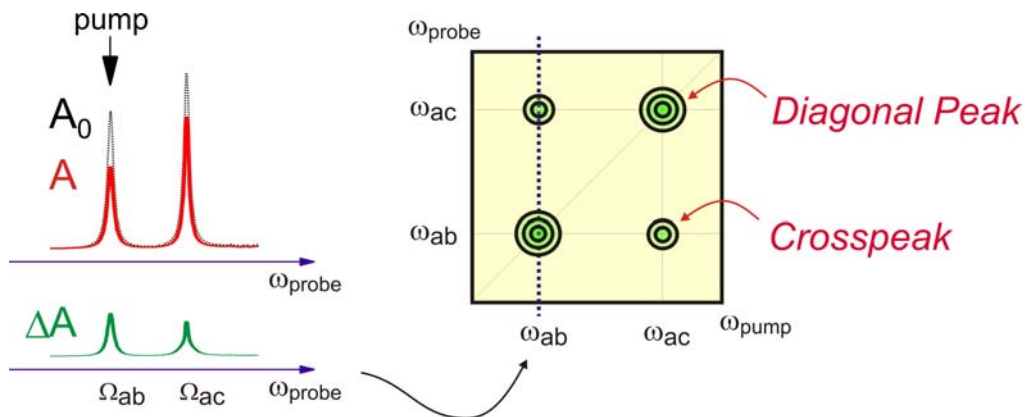


Imagine a double resonance (pump-probe) experiment in which we choose a tunable excitation frequency  $\omega_{pump}$ , and for each pump frequency we measure changes in the absorption spectrum as a function of  $\omega_{probe}$ . Generally speaking, we expect resonant excitation to induce a change of absorbance.

The question is: what do we observe if we pump at  $\omega_{ba}$  and probe at  $\omega_{ca}$ ? If nothing happens, then we can conclude that microscopically, there is no interaction between the degrees of freedom that give rise to the *ba* and *ca* transitions. However, a change of absorbance at  $\omega_{ca}$  indicates that in some manner the excitation of  $\omega_{ba}$  is correlated with  $\omega_{ca}$ . Microscopically, there is a coupling or chemical conversion that allows deposited energy to flow between the coordinates. Alternatively, we can say that the observed transitions occur between eigenstates whose character and energy encode molecular interactions between the coupled degrees of freedom (here  $\beta$  and  $\chi$ ):

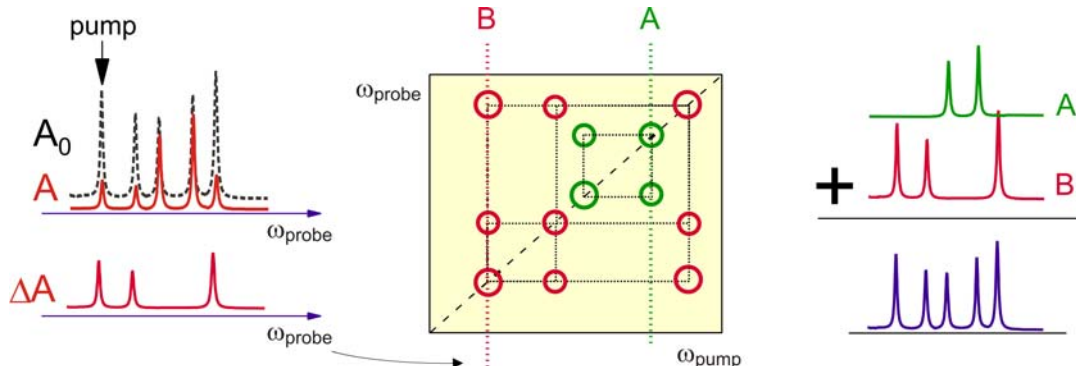


Now imagine that you perform this double resonance experiment measuring the change in absorption for all possible values of  $\omega_{pump}$  and  $\omega_{probe}$ , and plot these as a two-dimensional contour plot:<sup>1</sup>

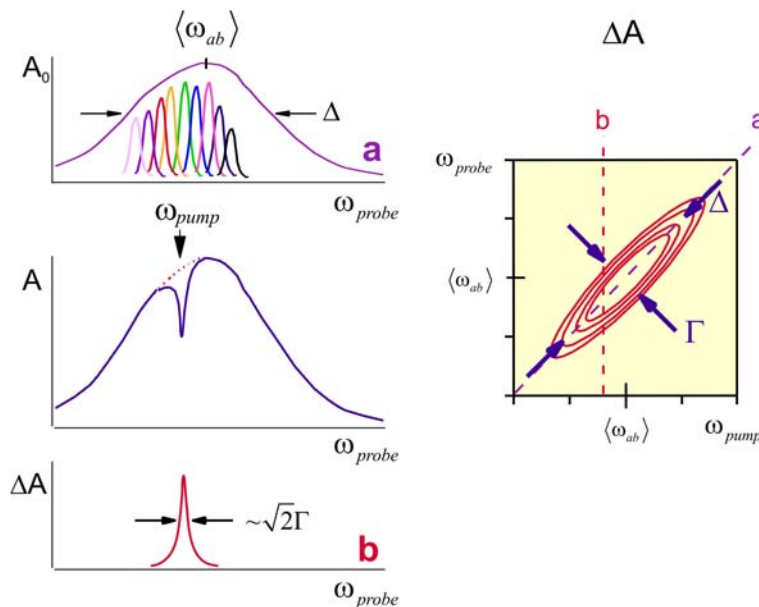


This is a two-dimensional spectrum that reports on the correlation of spectral features observed in the absorption spectrum. Diagonal peaks reflect the case where the same resonance is pumped and probed. Cross peaks indicate a cross-correlation that arises from pumping one feature and observing a change in the other. The principles of correlation spectroscopy in this form were initially developed in the area of magnetic resonance, but are finding increasing use in the areas of optical and infrared spectroscopy.

Double resonance analogies such as these illustrate the power of a two-dimensional spectrum to visualize the molecular interactions in a complex system with many degrees of freedom. Similarly, we can see how a 2D spectrum can separate components of a mixture through the presence or absence of cross peaks.



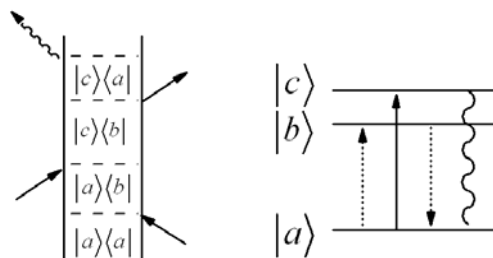
Also, it becomes clear how an inhomogeneous lineshape can be decomposed into the distribution of configurations, and the underlying dynamics within the ensemble. Take an inhomogeneous lineshape with width  $\Delta$  and mean frequency  $\langle\omega_{ab}\rangle$ , which is composed of a distribution of homogeneous transitions of width  $\Gamma$ . We will now subject the system to the same narrow band excitation followed by probing the differential absorption  $\Delta A$  at all probe frequencies.



Here we observe that the contours of a two-dimensional lineshape report on the inhomogeneous broadening. We observe that the lineshape is elongated along the diagonal axis ( $\omega_1 = \omega_3$ ). The diagonal linewidth is related to the inhomogeneous width  $\Delta$  whereas the antidiagonal width  $[\omega_1 + \omega_3 = \langle\omega_{ab}\rangle/2]$  is determined by the homogeneous linewidth  $\Gamma$ .

## 2D Spectroscopy from Third Order Response

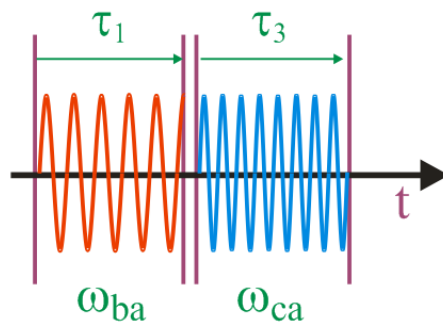
These examples indicate that narrow band pump-probe experiments can be used to construct 2D spectra, so in fact the third-order nonlinear response should describe 2D spectra. To describe these spectra, we can think of the excitation as a third-order process arising from a sequence of interactions with the system eigenstates. For instance, taking our initial example with three levels, one of the contributing factors is of the form  $R_2$ :



Setting  $\tau_2 = 0$  and neglecting damping, the response function is

$$R_2(\tau_1, \tau_3) = p_a |\mu_{ab}|^2 |\mu_{ac}|^2 e^{-i\omega_{ba}\tau_1 - i\omega_{ca}\tau_3} \quad (5.1)$$

The time domain behavior describes the evolution from one coherent state to another—driven by the light fields:



A more intuitive description is in the frequency domain, which we obtain by Fourier transforming eq. (5.1):

$$\begin{aligned} \tilde{R}_2(\omega_1, \omega_3) &= \int_{-\infty}^{\infty} \int_{-\infty}^{\infty} e^{i\omega_1\tau_1 + i\omega_3\tau_3} R_2(\tau_1, \tau_3) d\tau_1 d\tau_3 \\ &= p_a |\mu_{ab}|^2 |\mu_{ac}|^2 \langle \delta(\omega_3 - \omega_{ca}) \delta(\omega_1 - \omega_{ba}) \rangle \\ &\equiv p_a |\mu_{ab}|^2 |\mu_{ac}|^2 P(\omega_3, \tau_2; \omega_1) \end{aligned} \quad (5.2)$$

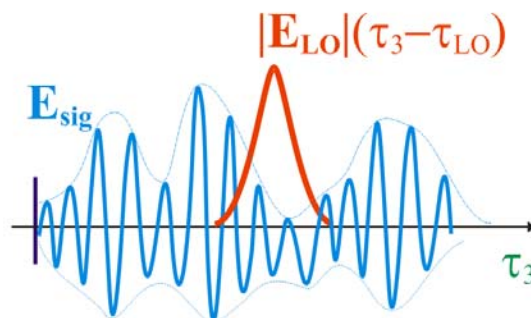
The function  $P$  looks just like the covariance  $\langle xy \rangle$  that describes the correlation of two variables  $x$  and  $y$ . In fact  $P$  is a joint probability function that describes the probability of exciting the system at  $\omega_{ba}$  and observing the system at  $\omega_{ca}$  (after waiting a time  $\tau_2$ ). In particular, this diagram describes the cross peak in the upper left of the initial example we discussed.

## Fourier transform spectroscopy

The last example underscores the close relationship between time and frequency domain representations of the data. Similar information to the frequency-domain double resonance

experiment is obtained by Fourier transformation of the coherent evolution periods in a time domain experiment with short broadband pulses.

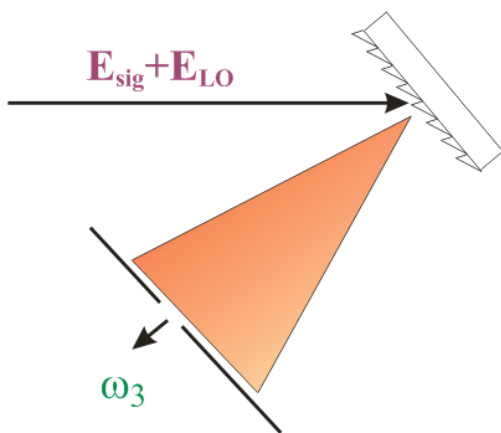
In practice, the use of Fourier transforms requires a phase-sensitive measure of the radiated signal field, rather than the intensity measured by photodetectors. This can be obtained by beating the signal against a reference pulse (or local oscillator) on a photodetector. If we measure the cross term between a weak signal and strong local oscillator:



$$\begin{aligned} \delta I_{LO}(\tau_{LO}) &= |E_{sig} + E_{LO}|^2 - |E_{LO}|^2 \\ &\approx 2 \operatorname{Re} \int_{-\infty}^{+\infty} d\tau_3 E_{sig}(\tau_3) E_{LO}(\tau_3 - \tau_{LO}) \end{aligned} \quad (5.3)$$

For a short pulse  $E_{LO}$ ,  $\delta I(\tau_{LO}) \propto E_{sig}(\tau_{LO})$ . By acquiring the signal as a function of  $\tau_1$  and  $\tau_{LO}$  we can obtain the time domain signal and numerically Fourier transform to obtain a 2D spectrum.

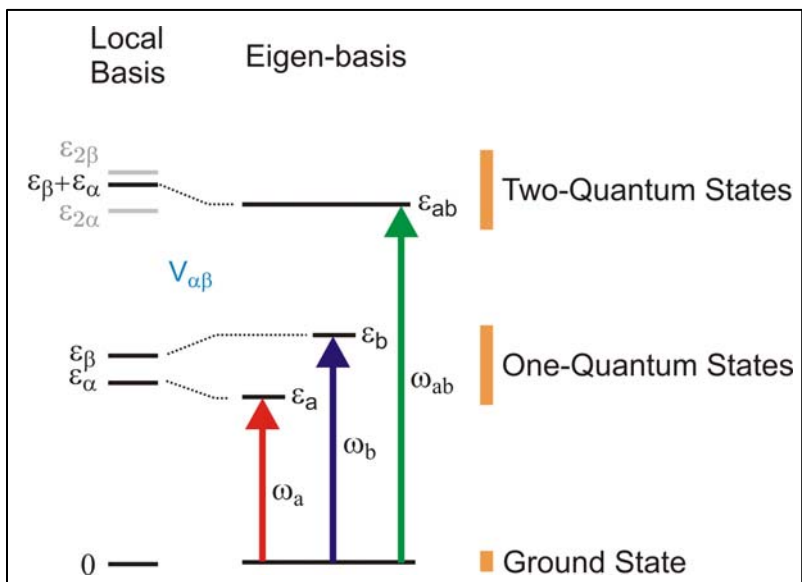
Alternatively, we can perform these operations in reverse order, using a grating or other dispersive optic to spatially disperse the frequency components of the signal. This is in essence an analog Fourier Transform. The interference between the spatially dispersed Fourier components of the signal and LO are subsequently detected.



$$\delta I(\omega_3) = \int |E_{LO}(\omega_3) + E_{sig}(\omega_3)|^2 - |E_{LO}(\omega_3)|^2$$

## Characterizing Couplings in 2D Spectra<sup>2</sup>

One of the unique characteristics of 2D spectroscopy is the ability to characterize molecular couplings. This allows one to understand microscopic relationships between different objects, and with knowledge of the interaction mechanism, determine the structure or reveal the dynamics of the system. To understand how 2D spectra report on molecular interactions, we will discuss the spectroscopy using a model for two coupled electronic or vibrational degrees of freedom. Since the 2D spectrum reports on the eigenstates of the coupled system, understanding the coupling between microscopic states requires a model for the eigenstates in the basis of the interacting coordinates of interest. Traditional linear spectroscopy does not provide enough constraints to uniquely determine these variables, but 2D spectroscopy provides this information through a characterization of two-quantum eigenstates. Since it takes less energy to excite one coordinate if a coupled coordinate already has energy in it, a characterization of the energy of the combination mode with one quantum of excitation in each coordinate provides a route to obtaining the coupling. This principle lies behind the use of overtone and combination band molecular spectroscopy to unravel anharmonic couplings.



The language for the different variables for the Hamiltonian of two coupled coordinates varies considerably by discipline. A variety of terms that are used are summarized below. We will use the underlined terms.

<i>System Hamiltonian</i> $H_S$	<i>Local or site basis</i> $(i,j)$	<i>Eigenbasis</i> $(a,b)$	<i>One-Quantum Eigenstates</i>	<i>Two-Quantum Eigenstates</i>
<u>Local mode Hamiltonian</u> Exciton Hamiltonian Frenkel Exciton Hamiltonian Coupled oscillators	<u>Sites</u> Local modes Oscillators Chromophores	<u>Eigenstates</u> Exciton states Delocalized states	<u>Fundamental</u> $v=0-1$ One-exciton states Exciton band	<u>Combination mode</u> or band Overtone Doubly excited states Biexciton Two-exciton states

The model for two coupled coordinates can take many forms. We will pay particular attention to a Hamiltonian that describes the coupling between two local vibrational modes  $i$  and  $j$  coupled through a bilinear interaction of strength  $J$ :

$$\begin{aligned} H_{vib} &= H_i + H_j + V_{i,j} \\ &= \frac{p_i^2}{2m_i} + V(q_i) + \frac{p_j^2}{2m_j} + V(q_j) + Jq_i q_j \end{aligned} \quad (5.4)$$

An alternate form cast in the ladder operators for vibrational or electronic states is the Frenkel exciton Hamiltonian

$$H_{vib,harmonic} \approx \hbar\omega_i (a_i^\dagger a_i) + \hbar\omega_j (a_j^\dagger a_j) + J(a_i^\dagger a_j + a_i a_j^\dagger). \quad (5.5)$$

$$H_{elec} = E_i a_i^\dagger a_i + E_j a_j^\dagger a_j + (J_{ij} a_i^\dagger a_j + c.c.) \quad (5.6)$$

The bi-linear interaction is the simplest form by which the energy of one state depends on the other. One can think of it as the leading term in the expansion of the coupling between the two local states. Higher order expansion terms are used in another common form, the cubic anharmonic coupling between normal modes of vibration

$$H_{vib} = \left( \frac{p_i^2}{2m_i} + \frac{1}{2} k_i q_i^2 + \frac{1}{6} g_{iii} q_i^3 \right) + \left( \frac{p_j^2}{2m_j} + \frac{1}{2} k_j q_j^2 + \frac{1}{6} g_{jjj} q_j^3 \right) + \left( \frac{1}{2} g_{ijj} q_i^2 q_j + \frac{1}{2} g_{iji} q_i q_j^2 \right). \quad (5.7)$$

The eigenstates and energy eigenvalues for the one-quantum states are obtained by diagonalizing the 2x2 matrix

$$H_S^{(1)} = \begin{pmatrix} E_{i=1} & J \\ J & E_{j=1} \end{pmatrix}. \quad (5.8)$$

$E_{i=1}$  and  $E_{j=1}$  are the one-quantum energies for the local modes  $q_i$  and  $q_j$ . These give the system energy eigenvalues

$$E_{a/b} = \Delta E \pm (\Delta E^2 + J^2)^{1/2} \quad (5.9)$$

$$\Delta E = \frac{1}{2}(E_{i=1} - E_{j=1}). \quad (5.10)$$

$E_a$  and  $E_b$  can be observed in the linear spectrum, but are not sufficient to unravel the three variables (site energies  $E_i$ ,  $E_j$  and coupling  $J$ ) relevant to the Hamiltonian; more information is needed.

For the purposes of 2D spectroscopy, the coupling is encoded in the two-quantum eigenstates. Since it takes less energy to excite a vibration  $|i\rangle$  if a coupled mode  $|j\rangle$  already has energy, we can characterize the strength of interaction from the system eigenstates by determining the energy of the combination mode  $E_{ab}$  relative to the sum of the fundamentals:

$$\Delta_{ab} = E_a + E_b - E_{ab}. \quad (5.11)$$

In essence, with a characterization of  $E_{ab}, E_a, E_b$  one has three variables that constrain  $E_i, E_j, J$ . The relationship between  $\Delta_{ab}$  and  $J$  depends on the model.

Working specifically with the vibrational Hamiltonian eq. (5.4), there are three two-quantum states that must be considered. Expressed as product states in the two local modes these are  $|i, j\rangle = |20\rangle, |02\rangle$ , and  $|11\rangle$ . The two-quantum energy eigenvalues of the system are obtained by diagonalizing the 3x3 matrix

$$H_S^{(2)} = \begin{pmatrix} E_{i=2} & 0 & \sqrt{2}J \\ 0 & E_{j=2} & \sqrt{2}J \\ \sqrt{2}J & \sqrt{2}J & E_{i=1} + E_{j=1} \end{pmatrix} \quad (5.12)$$

Here  $E_{i=2}$  and  $E_{j=2}$  are the two-quantum energies for the local modes  $q_i$  and  $q_j$ . These are commonly expressed in terms of  $\delta E_i$ , the anharmonic shift of the  $i=1-2$  energy gap relative to the  $i=0-1$  one-quantum energy:

$$\begin{aligned} \delta E_i &= (E_{i=1} - E_{i=0}) - (E_{i=2} - E_{i=1}) \\ \delta \omega_i &= \omega_{10}^i - \omega_{21}^i \end{aligned} \quad (5.13)$$

Although there are analytical solutions to eq. (5.12), it is more informative to examine solutions in two limits. In the strong coupling limit ( $J \gg \Delta E$ ), one finds

$$\Delta_{ab} = J. \quad (5.14)$$

For vibrations with the same anharmonicity  $\delta E$  with weak coupling between them ( $J \ll \Delta E$ ), perturbation theory yields

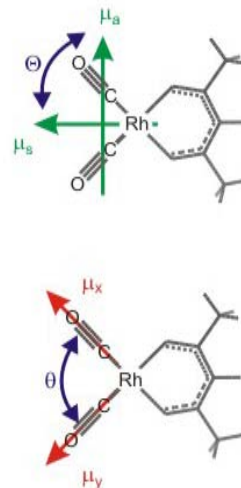
$$\Delta_{ab} = \delta E \frac{J^2}{\Delta E^2}. \quad (5.15)$$

This result is similar to the perturbative solution for weakly coupled oscillators of the form given by eq. (5.7)

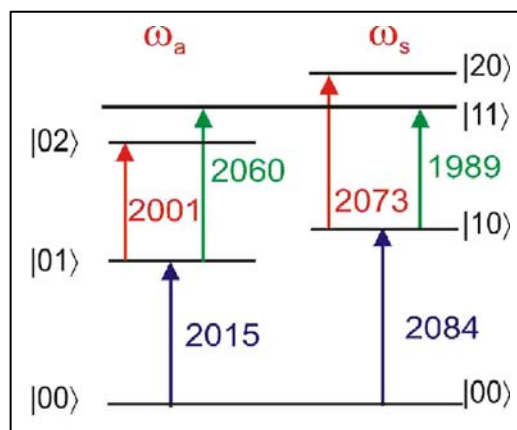
$$\Delta_{ab} = g_{ij}^2 \left( \frac{4E_i}{E_j^2 - 4E_i^2} \right) + g_{ij}^2 \left( \frac{4E_j}{E_i^2 - 4E_j^2} \right). \quad (5.16)$$

## EXAMPLE

So, how do these variables present themselves in 2D spectra? Here it is helpful to use a specific example: the strongly coupled carbonyl vibrations of  $\text{Rh}(\text{CO})_2(\text{acac})$  or RDC. For the purpose of 2D spectroscopy with infrared fields resonant with the carbonyl transitions, there are six quantum states (counting the ground state) that must be considered. Coupling between the two degenerate CO stretches leads to symmetric and anti-symmetric one-quantum eigenstates, which are more commonly referred to by their normal mode designations: the symmetric and asymmetric stretching vibrations. For  $n=2$  coupled vibrations, there are  $n(n-1)/2 = 3$  two-quantum eigenstates. In the normal mode designation, these are the first overtones of the symmetric and asymmetric modes and the combination band. This leads to a six level system for the system eigenstates, which we designate by the number of quanta in the symmetric and asymmetric stretch:  $|00\rangle, |s\rangle = |10\rangle, |a\rangle = |01\rangle, |2s\rangle = |20\rangle, |2a\rangle = |02\rangle$ , and  $|sa\rangle = |11\rangle$ . For a model electronic system, there are four essential levels that need to be considered, since Fermi statistics does not allow two electrons in the same state:  $|00\rangle, |10\rangle, |01\rangle$ , and  $|11\rangle$ .



We now calculate the nonlinear third-order response for this six-level system, assuming that all of the population is initially in the ground state. To describe a double-resonance or Fourier transform 2D correlation spectrum in the variables  $\omega_1$  and  $\omega_3$ , include all terms relevant to pump-probe experiments:  $-k_1 + k_2 + k_3$  ( $S_I$ , rephasing) and  $k_1 - k_2 + k_3$  ( $S_{II}$ , non-rephasing). After summing over many interaction permutations using the phenomenological propagator, keeping only dipole allowed transitions with  $\pm 1$



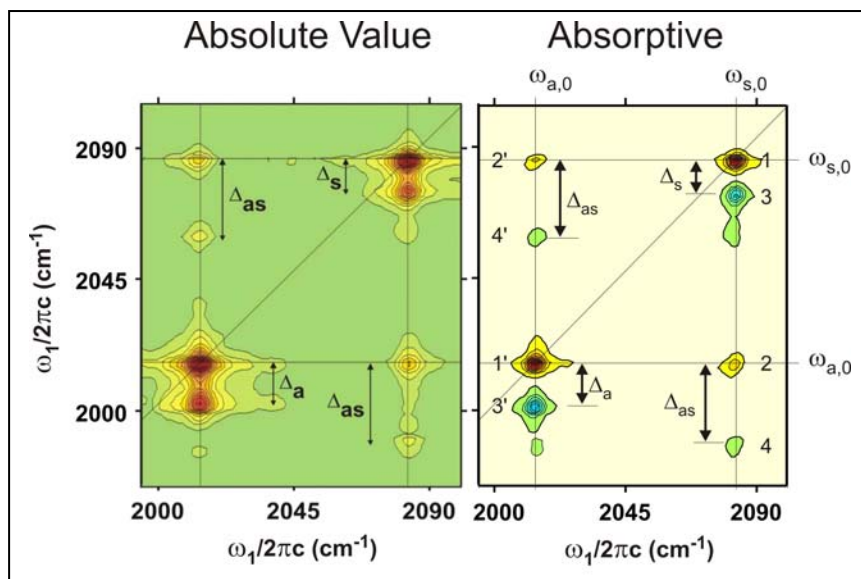
quantum, we find that we expect eight resonances in a 2D spectrum. For the case of  $S_I$

$$\begin{aligned}
 S_I(\omega_1, \omega_3) = & \frac{2|\mu_{s,0}|^4}{\left[ i(\omega_1 + \omega_{s,0}) + \Gamma_{s,0} \right] \left[ i(\omega_3 - \omega_{s,0}) + \Gamma_{s,0} \right]} + \frac{2|\mu_{a,0}|^4}{\left[ i(\omega_1 + \omega_{a,0}) + \Gamma_{a,0} \right] \left[ i(\omega_3 - \omega_{a,0}) + \Gamma_{a,0} \right]} \\
 & + \frac{2|\mu_{a,0}|^2 |\mu_{s,0}|^2}{\left[ i(\omega_1 + \omega_{s,0}) + \Gamma_{s,0} \right] \left[ i(\omega_3 - \omega_{a,0}) + \Gamma_{a,0} \right]} + \frac{2|\mu_{a,0}|^2 |\mu_{s,0}|^2}{\left[ i(\omega_1 + \omega_{a,0}) + \Gamma_{a,0} \right] \left[ i(\omega_3 - \omega_{s,0}) + \Gamma_{s,0} \right]} \\
 & - \frac{|\mu_{s,0}|^2 |\mu_{2s,s}|^2}{\left[ i(\omega_1 + \omega_{s,0}) + \Gamma_{s,0} \right] \left[ i(\omega_3 - \omega_{s,0} + \Delta_s) + \Gamma_{2s,s} \right]} - \frac{|\mu_{a,0}|^2 |\mu_{2a,a}|^2}{\left[ i(\omega_1 + \omega_{a,0}) + \Gamma_{a,0} \right] \left[ i(\omega_3 - \omega_{a,0} + \Delta_a) + \Gamma_{2a,a} \right]} \\
 & - \frac{|\mu_{s,0}|^2 |\mu_{as,s}|^2 + \mu_{0,s} \mu_{a,0} \mu_{as,a} \mu_{s,as}}{\left[ i(\omega_1 + \omega_{s,0}) + \Gamma_{s,0} \right] \left[ i(\omega_3 - \omega_{a,0} + \Delta_{as}) + \Gamma_{as,s} \right]} - \frac{|\mu_{a,0}|^2 |\mu_{as,a}|^2 + \mu_{0,a} \mu_{s,0} \mu_{as,s} \mu_{a,as}}{\left[ i(\omega_1 + \omega_{a,0}) + \Gamma_{a,0} \right] \left[ i(\omega_3 - \omega_{s,0} + \Delta_{as}) + \Gamma_{as,a} \right]} \\
 \equiv & \mathbf{1 + 1' + 2 + 2' + 3 + 3' + 4 + 4'}
 \end{aligned} \tag{5.17}$$

To discuss these peaks we examine how they appear in the experimental Fourier transform 2D IR spectrum of RDC, here plotted both as in differential absorption mode and absolute value mode. We note that there are eight peaks, labeled according to the terms i eq. (5.17) from which they arise. Each peak specifies a sequence of interactions with the system eigenstates, with excitation at a particular  $\omega_1$  and detection at given  $\omega_3$ . Notice that in the excitation dimension  $\omega_1$  all of the peaks lie on one of the fundamental frequencies. Along the detection axis  $\omega_3$  resonances are seen at all six one-quantum transitions present in our system.

More precisely, there are four features: two diagonal and two cross peaks each of which are split into a pair. The positive diagonal and cross peak features represent evolution on the fundamental transitions,

while the split negative features arise from propagation in the two-quantum manifold. The diagonal peaks represent a sequence of interactions with the field that leaves the coherence on the same transition during both

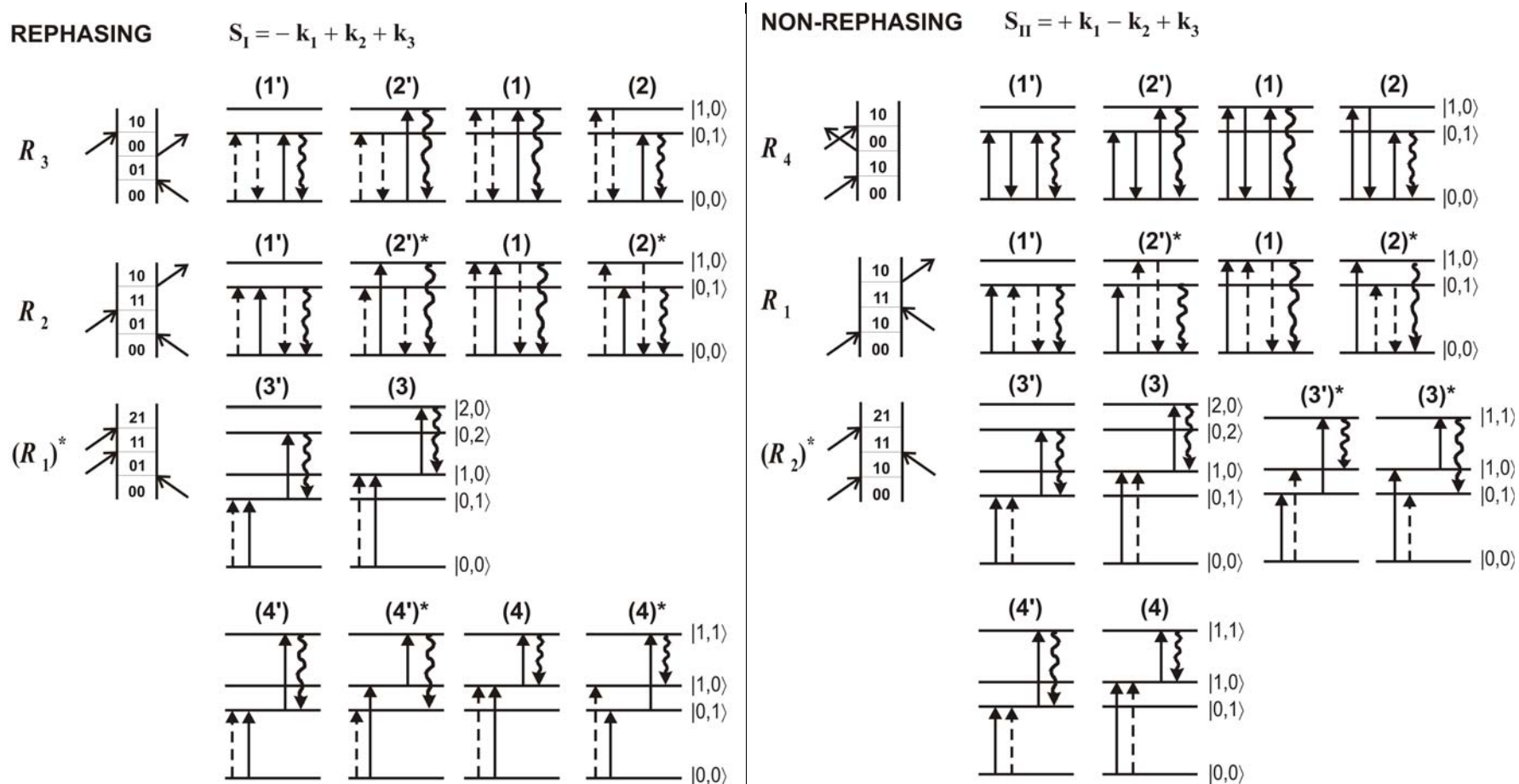


periods, where as the split peak represents promotion from the fundamental to the overtone during detection. The overtone is anharmonically shifted, and therefore the splitting between the peaks,  $\Delta_a, \Delta_s$ , gives the diagonal anharmonicity. The cross peaks arise from the transfer of excitation from one fundamental to the other, while the shifted peak represents promotion to the combination band for detection. The combination band is shifted in frequency due to coupling between the two modes, and therefore the splitting between the peaks in the off-diagonal features  $\Delta_{as}$  gives the off-diagonal anharmonicity.

Notice for each split pair of peaks, that in the limit that the anharmonicity vanishes, the two peaks in each feature would overlap. Given that they have opposite sign, the peaks would destructively interfere and vanish for a harmonic system. This is a manifestation of the rule that a nonlinear response vanishes for a harmonic system. So, in fact, a 2D spectrum will have signatures of whatever types of vibrational interactions lead to imperfect interference between these two contributions. Nonlinearity of the transition dipole moment will lead to imperfect cancellation of the peaks at the amplitude level, and nonlinear coupling with a bath will lead to different lineshapes for the two features.

With an assignment of the peaks in the spectrum, one has mapped out the energies of the one- and two-quantum system eigenstates. These eigenvalues act to constrain any model that will be used to interpret the system. One can now evaluate how models for the coupled vibrations match the data. For instance, when fitting the RDC spectrum to the Hamiltonian in eq. (5.4) for two coupled anharmonic local modes with a potential of the form  $V(q_i) = \frac{1}{2}k_i q_i^2 + \frac{1}{6}g_{iii}q_i^3$ , we obtain  $\hbar\omega_{10}^i = \hbar\omega_{10}^j = 2074 \text{ cm}^{-1}$ ,  $J_{ij} = 35 \text{ cm}^{-1}$ , and  $g_{iii} = g_{jjj} = 172 \text{ cm}^{-1}$ . Alternatively, we can describe the spectrum through eq. (5.7) as symmetric and asymmetric normal modes with diagonal and off-diagonal anharmonicity. This leads to  $\hbar\omega_{10}^a = 2038 \text{ cm}^{-1}$ ,  $\hbar\omega_{10}^s = 2108 \text{ cm}^{-1}$ ,  $g_{aaa} = g_{sss} = 32 \text{ cm}^{-1}$ , and  $g_{ssa} = g_{aas} = 22 \text{ cm}^{-1}$ . Provided that one knows the origin of the coupling and its spatial or angular dependence, one can use these parameters to obtain a structure.

**Appendix: Third Order Diagrams Corresponding to Peaks in a 2D Spectrum of Coupled Vibrations**



\*Diagrams that do not contribute to double-resonance experiments, but do contribute to Fourier-transform measurements.

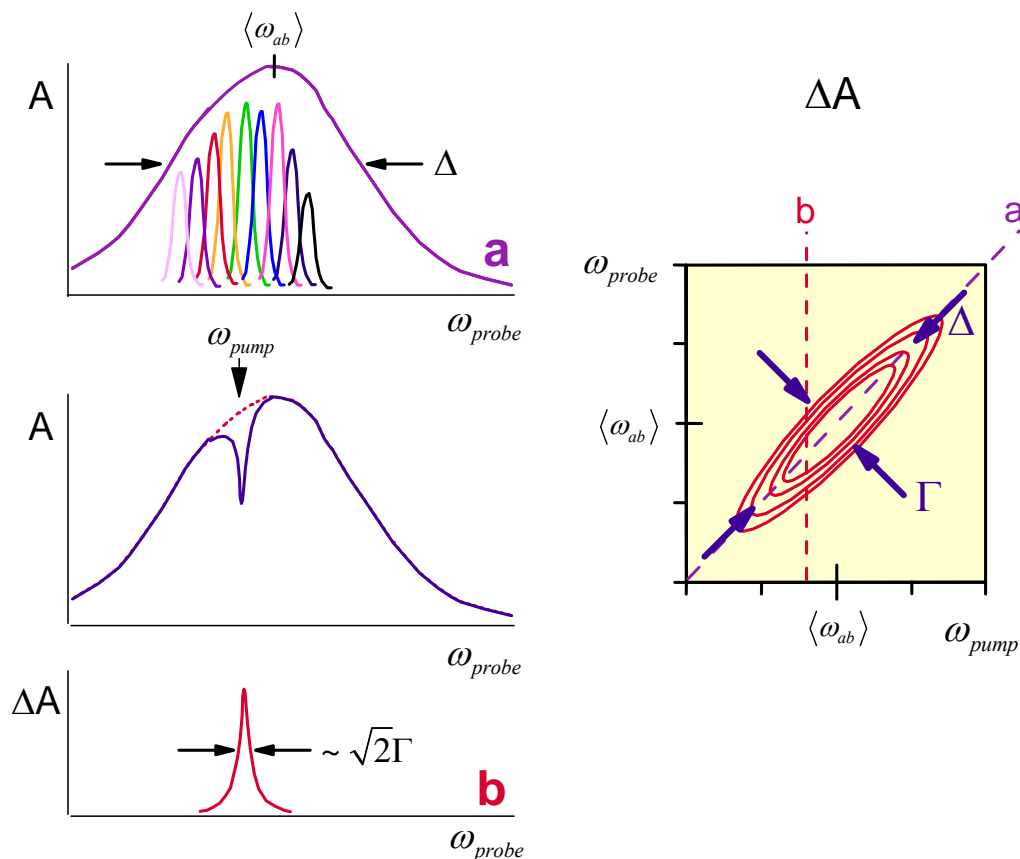
Rephasing diagrams correspond to the terms in eq. (5.17).

Using a phenomenological propagator, the  $S_{II}$  non-rephasing diagrams lead to the following expressions for the eight peaks in the 2D spectrum.

$$\begin{aligned}
S_{II}(\omega_1, \omega_3) = & \frac{2|\mu_{s,0}|^4}{[-i(\omega_1 - \omega_{s,0}) + \Gamma_{s,0}][i(\omega_3 - \omega_{s,0}) + \Gamma_{s,0}]} + \frac{2|\mu_{a,0}|^4}{[-i(\omega_1 - \omega_{a,0}) + \Gamma_{a,0}][i(\omega_3 - \omega_{a,0}) + \Gamma_{a,0}]} \\
& + \frac{2|\mu_{a,0}|^2|\mu_{s,0}|^2}{[-i(\omega_1 - \omega_{s,0}) + \Gamma_{s,0}][i(\omega_3 - \omega_{a,0}) + \Gamma_{a,0}]} + \frac{2|\mu_{a,0}|^2|\mu_{s,0}|^2}{[-i(\omega_1 - \omega_{a,0}) + \Gamma_{a,0}][i(\omega_3 - \omega_{s,0}) + \Gamma_{s,0}]} \\
& - \frac{|\mu_{s,0}|^2|\mu_{2s,s}|^2 + \mu_{s,0}\mu_{0,a}\mu_{as,s}\mu_{a,as}}{[-i(\omega_1 - \omega_{s,0}) + \Gamma_{s,0}][i(\omega_3 - \omega_{s,0} + \Delta_s) + \Gamma_{2s,s}]} - \frac{|\mu_{a,0}|^2|\mu_{2a,a}|^2 + \mu_{a,0}\mu_{0,s}\mu_{as,a}\mu_{s,as}}{[-i(\omega_1 - \omega_{a,0}) + \Gamma_{a,0}][i(\omega_3 - \omega_{a,0} + \Delta_a) + \Gamma_{2a,a}]} \quad (5.18) \\
& - \frac{|\mu_{s,0}|^2|\mu_{as,s}|^2}{[-i(\omega_1 - \omega_{s,0}) + \Gamma_{s,0}][i(\omega_3 - \omega_{a,0} + \Delta_{as}) + \Gamma_{as,s}]} - \frac{|\mu_{a,0}|^2|\mu_{as,a}|^2}{[-i(\omega_1 - \omega_{a,0}) + \Gamma_{a,0}][i(\omega_3 - \omega_{s,0} + \Delta_{as}) + \Gamma_{as,a}]} \\
\equiv & \mathbf{1 + 1' + 2 + 2' + 3 + 3' + 4 + 4'}
\end{aligned}$$

## Two-dimensional spectroscopy to characterize spectral diffusion

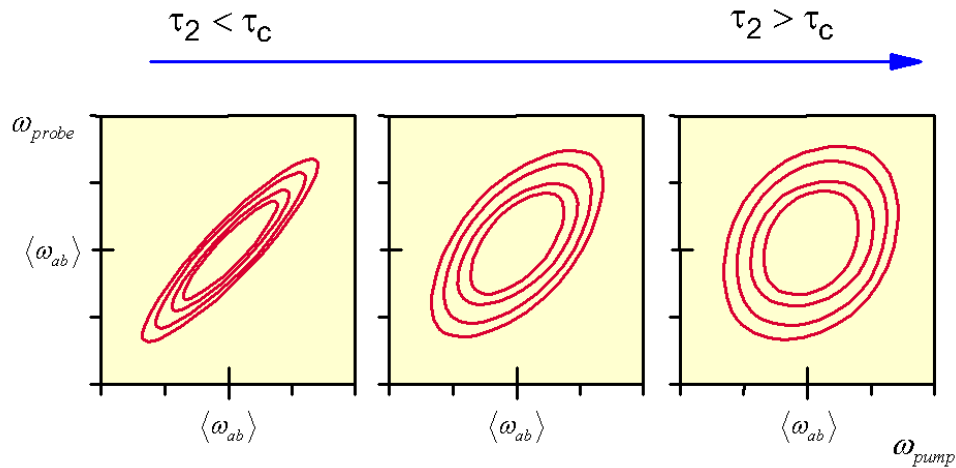
A more intuitive, albeit difficult, approach to characterizing spectral diffusion is with a two-dimensional correlation technique. Returning to our example of a double resonance experiment, let's describe the response from an inhomogeneous lineshape with width  $\Delta$  and mean frequency  $\langle\omega_{ab}\rangle$ , which is composed of a distribution of homogeneous transitions of width  $\Gamma$ . We will now subject the system to excitation by a narrow band pump field, and probe the differential absorption  $\Delta A$  at all probe frequencies. We then repeat this for all pump frequencies:



In constructing a two-dimensional representation of this correlation spectrum, we observe that the observed lineshape is elongated along the diagonal axis ( $\omega_1=\omega_3$ ). The diagonal linewidth is related to the inhomogeneous width  $\Delta$  whereas the antidiagonal width  $[\omega_1 + \omega_3 = \langle\omega_{ab}\rangle/2]$  is determined by the homogeneous linewidth  $\Gamma$ .

For the system exhibiting spectral diffusion, we recognize that we can introduce a waiting time  $\tau_2$  between excitation and detection, which provides a controlled period over which the

system can evolve. One can see that when  $\tau_2$  varies from much less to much greater than the correlation time,  $\tau_c$ , that the lineshape will gradually become symmetric.



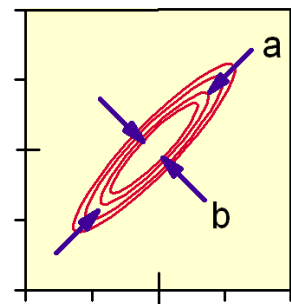
This reflects the fact that at long times the system excited at any one frequency can be observed at any other with equilibrium probability. That is, the correlation between excitation and detection frequencies vanishes.

$$\begin{aligned} & \sum_{ij} \langle \delta(\omega_1 - \omega_{eg}^{(i)}) \delta(\omega_3 - \omega_{eg}^{(j)}) \rangle \\ & \rightarrow \sum_{ij} \langle \delta(\omega_1 - \omega_{eg}^{(i)}) \rangle \langle \delta(\omega_3 - \omega_{eg}^{(j)}) \rangle \end{aligned} \tag{5.19}$$

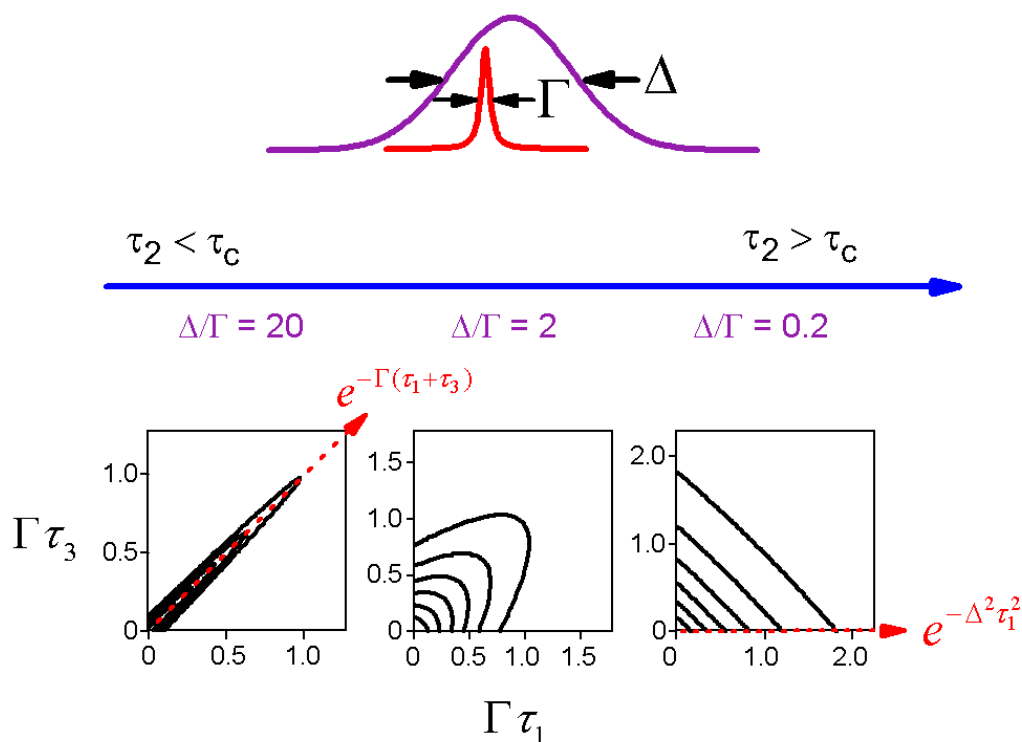
To characterize the energy gap correlation function, we choose a metric that describes the change as a function of  $\tau_2$ . For instance, the ellipticity

$$E(\tau_2) = \frac{a^2 - b^2}{a^2 + b^2} \tag{5.20}$$

is directly proportional to  $C_{eg}(\tau)$ .



The photon echo experiment is the time domain version of this double-resonance or hole burning experiment. If we examine  $R_2$  in the inhomogeneous and homogeneous limits, we can plot the polarization envelope as a function of  $\tau_1$  and  $\tau_3$ .



In the inhomogeneous limit, an echo ridge decaying as  $e^{-\Gamma t}$  extends along  $\tau_1 = \tau_3$ . It decays with the inhomogeneous distribution in the perpendicular direction. In the homogeneous limit, the response is symmetric in the two time variables. Fourier transformation allows these envelopes to be expressed as the lineshapes above. Here again  $\tau_2$  is a control variable to allow us to characterize  $C_{eg}(\tau)$  through the change in echo profile or lineshape.

<sup>1</sup> Here we use the right-hand rule convention for the frequency axes, in which the pump or excitation frequency is on the horizontal axis and the probe or detection frequency is on the vertical axis. Different conventions are being used, which does lead to confusion. We note that the first presentations of two-dimensional spectra in the case of 2D Raman and 2D IR spectra used a RHR convention, whereas the first 2D NMR and 2D electronic measurements used the LHR convention.

<sup>2</sup> Khalil M, Tokmakoff A. "Signatures of vibrational interactions in coherent two-dimensional infrared spectroscopy." *Chem Phys*. 2001;266(2-3):213-30; Khalil M, Demirdöven N, Tokmakoff A. "Coherent 2D IR Spectroscopy: Molecular structure and dynamics in solution." *J Phys Chem A*. 2003;107(27):5258-79; Woutersen S, Hamm P. Nonlinear two-dimensional vibrational spectroscopy of peptides. *J Phys: Condens Mat*. 2002;14:1035-62.